Int. J. Solids Structures Vol. 24, No. 11, pp. 1141–1158, 1988
Printed in Great Britain.

0020-7683/88 $3.00+ .00

ASYMPTOTIC CRACK TIP FIELDS FOR DYNAMIC FRACTURE OF LINEAR STRAIN-HARDENING SOLIDS

SÖREN ÖSTLUND and PETER GUDMUNDSON
Department of Strength of Materials and Solid Mechanics, The Royal Institute of Technology, S-100 44 Stockholm, Sweden

(*Received* 2 *February* 1988)

Abstract—Asymptotic crack tip fields, for dynamic crack propagation in an elastic–plastic material, have been calculated. The material is characterized by J_2 flow theory with linear-strain hardening. The possibility of plastic reloading on the crack flank is taken into account. Numerical results for the strength of the crack tip singularity, the angular positions of elastic unloading and possible plastic reloading regions, and the angular variation of the stress and velocity fields, are presented as functions of the crack tip speed and the ratio between tangent modulus and elastic modulus. Calculations have been performed for crack tip speeds below a certain limit velocity which depends on the tangent modulus and the loading conditions. The different loading modes which have been studied are modes I and II (plane strain and plane stress) and mode III (antiplane strain).

1. INTRODUCTION

During the last years there has been a great interest in asymptotic solutions, for crack propagation problems. Knowledge of the stress and deformation fields near a propagating crack tip is of importance for the understanding of fracture mechanisms. Especially asymptotic solutions for dynamic problems, i.e. when inertia effects are of importance in the analysis, are still not completely developed.

Asymptotic solutions for dynamic crack propagation in elastic–perfectly plastic solids have been investigated by Slepyan (1976), and Achenbach and Dunayevsky (1981) who considered both the antiplane strain and the in-plane strain problem. The mode I solution of Achenbach and Dunayevsky was further extended by Leighton *et al.* (1987). Lam and Freund (1985) studied the same problem by a convective finite element method. Their results were consistent with the solution given by Achenbach and Dunayevsky for low crack tip speeds. A mode II solution for elastic–perfectly plastic solids was presented by Lo (1982).

Dynamic crack propagation in linear strain-hardening materials was examined by Achenbach and Kanninen (1978) (referred to as AK in the sequel), who studied mode III crack growth, and Achenbach *et al.* (1981) (referred to as AKP in the sequel), who considered the plane stress and plane strain (mode I) problems. However, in these two papers the possibility of plastic reloading on the crack flanks was neglected. In this paper the problems considered by AK and AKP will be reanalysed by including the possibility of reverse plastic flow on the crack flanks. For completeness, although of minor technical interest, results for mode II plane stress and plane strain crack growth will also be presented.

The present procedure is based on the work of AKP but modified with conditions for plastic reloading. It is assumed that in front of the crack tip there exists a region of plastic loading. At a certain angle θ_1, defining the location of a straight boundary line, elastic unloading will occur. Another angle θ_2, where $\theta_2 > \theta_1$, defines the location for possible plastic reloading (Fig. 1). For some loading conditions, a second unloading is possible at an angle θ_3 and a second plastic reloading may occur at an angle denoted by θ_4.

The stress and velocity fields in the plastic loading regions are determined by numerical integration in the θ-direction of a system of non-linear differential equations. In the elastic unloading region, the solution is given in a general form specified by using continuity conditions at the boundary lines between plastic loading regions and elastic unloading regions. It was only possible to obtain results for values of the crack tip velocity less than a certain limit speed. At this limit speed, which depends on the loading conditions and the slope of the effective stress–strain curve at large strains, the governing equations in the

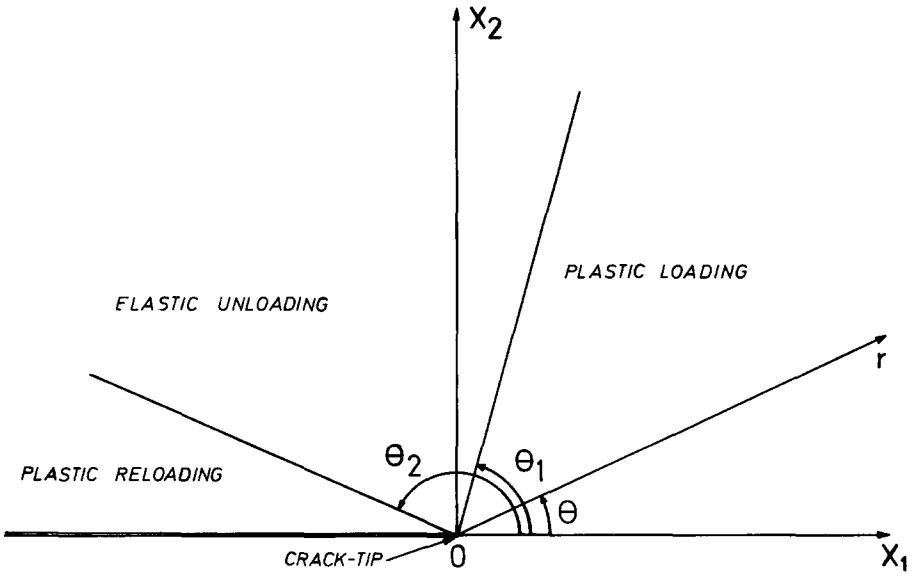

Fig. 1. Coordinate system and definition of unloading and reloading angles.

plastic loading zone become singular at a certain angle. This is due to a change in character of the equations from elliptic to hyperbolic as discussed by Achenbach *et al.* (1979).

To check the accuracy of the results, comparisons were made with the results of AK and AKP. Additional confidence was also attained by comparing calculations for low crack tip speeds to Ponte Castaneda's (1987) results for quasi-static crack growth.

2. PLANE STRAIN (MODE I)

2.1. *Plastic loading*

The asymptotic fields will be studied in a Cartesian coordinate system the origin O of which is attached to the moving crack tip, and oriented so that the x_3-axis coincides with the crack front and the x_1-axis is in the direction of crack advance (Fig. 1). The non-zero stresses are σ_{11}, σ_{22}, σ_{12} $(=\sigma_{21})$ and σ_{33}. The relevant displacement components are $u_1(x_1, x_2, t)$ and $u_2(x_1, x_2, t)$, where t is time.

The equations of motion are

$$\sigma_{\gamma\delta,\delta} = \rho\ddot{u}_\gamma \tag{1}$$

where ρ is the density and $(\ddot{})$ the second-order material time derivative. In the following, Greek subscripts have the values 1, 2 whereas Latin subscripts have the values 1, 2, 3. The

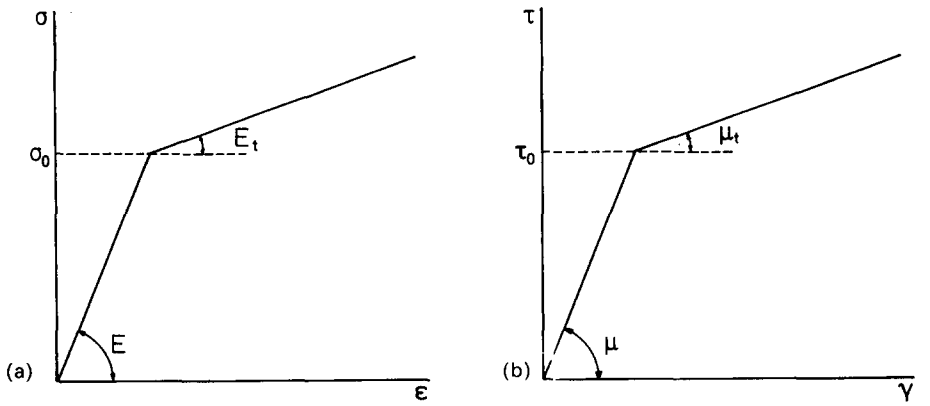

Fig. 2. Stress–strain relations for simple tension and pure shear.

constitutive equations in the plastic loading zone, taking into account strain hardening characterized by J_2 flow theory and a bilinear effective stress–strain curve (Fig. 2(a)), are

$$E_t\dot{\varepsilon}_{ij} = \alpha[(1+\nu)\dot{\sigma}_{ij} - \nu\dot{\sigma}_{kk}\delta_{ij}] + \tfrac{3}{2}\sigma_e^{-1}(1-\alpha)s_{ij}\dot{\sigma}_e \tag{2}$$

where $\dot{\varepsilon}_{ij}$ is the strain-rate tensor, $\dot{\sigma}_{ij}$ the stress-rate tensor, δ_{ij} the Kronecker δ-symbol, s_{ij} the stress deviator and ν is Poisson's ratio

$$\alpha = E_t/E \tag{3}$$

where E is Young's modulus and E_t the tangential stiffness of the bilinear stress–strain relation for stresses in excess of σ_0 (Fig. 2(a)).

The effective stress, σ_e, is defined as

$$\sigma_e = (\tfrac{3}{2}s_{ij}s_{ij})^{1/2}. \tag{4}$$

Introducing polar coordinates, r and θ (Fig. 1), asymptotic solutions of the general form

$$\dot{u}_\gamma = Kv\dot{U}_\gamma(\theta)r^s \tag{5}$$

are sought, where K is an undetermined amplitude factor, v the crack tip velocity and $\dot{U}_\gamma(\theta)$ and s are to be determined. In an asymptotic analysis only the most singular terms need to be retained. This means that in the material time derivative $(\dot{})$, $\partial/\partial t$ is negligible compared to $-v\partial/\partial x_1$ and

$$(\dot{}) \approx -v\frac{\partial(\ )}{\partial x_1}. \tag{6}$$

Two relations which will be used frequently in the sequel are

$$\frac{\partial}{\partial x_1} = \cos\theta\frac{\partial}{\partial r} - \frac{\sin\theta}{r}\frac{\partial}{\partial\theta}$$

and

$$\frac{\partial}{\partial x_2} = \sin\theta\frac{\partial}{\partial r} + \frac{\cos\theta}{r}\frac{\partial}{\partial\theta}. \tag{7}$$

By definition the following expressions for the stresses and the stress rates are introduced:

$$\{\sigma_{ij}, \sigma_e, s_{ij}\} = KE\{\Sigma_{ij}(\theta), \Sigma_e(\theta), S_{ij}(\theta)\}r^s \tag{8}$$

$$\{\dot{\sigma}_{ij}, \dot{\sigma}_e, \dot{s}_{ij}\} = KEv\{\dot{\Sigma}_{ij}(\theta), \dot{\Sigma}_e(\theta), \dot{S}_{ij}(\theta)\}r^{s-1}. \tag{9}$$

Equations (6) and (7) give

$$\dot{\Sigma}_{ij} = -s\Sigma_{ij}\cos\theta + \Sigma'_{ij}\sin\theta \tag{10}$$

and similar expressions for $\dot{\Sigma}_e$ and $\dot{S}_{ij}$. Here $(\ )'$ denotes $\mathrm{d}(\ )/\mathrm{d}\theta$. Also

$$S_{ij} = \Sigma_{ij} - \tfrac{1}{3}\Sigma_{kk}\delta_{ij} \tag{11}$$

$$\Sigma_e = (\tfrac{3}{2}S_{ij}S_{ij})^{1/2}. \tag{12}$$

By introducing the displacement rate, eqn (5), the stresses and stress rates, eqns (8) and

(9), into the equations of motion (1) and the constitutive equations (2), it is possible by using eqns (6), (7), (10) and (11) to formulate a non-linear system of differential equations

$$\mathbf{D}(S_{ij})\mathbf{y}' + \mathbf{R}\mathbf{y} = \mathbf{0} \tag{13}$$

where

$$\mathbf{y}^{\mathrm{T}} = [\dot{U}_1, \dot{U}_2, \dot{\Sigma}_{11}, \dot{\Sigma}_{22}, \dot{\Sigma}_{12}, \dot{\Sigma}_{33}]. \tag{14}$$

In the derivation of eqn (13) it is convenient to introduce a dimensionless crack tip velocity $\beta = v/c$, where $c = \sqrt{(E/\rho)}$. The details and the elements of matrices **D** and **R** are given in AKP. The last equation in eqn (13) is obtained by using the plane strain condition, $\dot{\varepsilon}_{33} = 0$.

2.2. *Elastic unloading*

The solution for the elastic unloading zone follows from AKP. For plane strain the displacement rate must satisfy

$$(\lambda+\mu)\dot{u}_{\gamma,\gamma\delta} + \mu\dot{u}_{\delta,\gamma\gamma} = \rho(\ddot{u}_\delta) \tag{15}$$

where λ and μ are Lamé's elastic constants. By introducing displacement-rate potentials $\dot{\phi}(x_1, x_2, t)$ and $\dot{\psi}(x_1, x_2, t)$ through

$$\dot{u}_1 = \frac{\partial\dot{\phi}}{\partial x_1} + \frac{\partial\dot{\psi}}{\partial x_2}; \quad \dot{u}_2 = \frac{\partial\dot{\phi}}{\partial x_2} - \frac{\partial\dot{\psi}}{\partial x_1} \tag{16}$$

$\dot{u}_1$ and $\dot{u}_2$ will satisfy eqn (15) if $\dot{\phi}$ and $\dot{\psi}$ are solutions of the wave equations

$$\dot{\phi}_{,\gamma\gamma} = \frac{1}{C_{\mathrm{L}}^2}\ddot{\phi}, \quad C_{\mathrm{L}}^2 = \frac{(\lambda+2\mu)}{\rho} \tag{17}$$

$$\dot{\psi}_{,\gamma\gamma} = \frac{1}{C_{\mathrm{T}}^2}\ddot{\psi}, \quad C_{\mathrm{T}}^2 = \frac{\mu}{\rho}. \tag{18}$$

Here, C_{L} and C_{T} denote the longitudinal and transverse elastic wave speeds, respectively. In the following it is convenient to introduce $\beta_{\mathrm{T}} = v/C_{\mathrm{T}}$ and $\beta_{\mathrm{L}} = v/C_{\mathrm{L}}$. It is possible to show that solutions to eqns (17) and (18), can be written as

$$\dot{\phi} = Kv\dot{\Phi}(\beta_{\mathrm{L}}, \theta)r^p \tag{19}$$

$$\dot{\psi} = Kv\dot{\Psi}(\beta_{\mathrm{T}}, \theta)r^p \tag{20}$$

where

$$\dot{\Phi}(\beta_{\mathrm{L}}, \theta) = (1-\beta_{\mathrm{L}}^2 \sin^2\theta)^{p/2}[A \sin\{p(\varepsilon-\pi)\} + B\cos\{p(\varepsilon-\pi)\}] \tag{21}$$

$$\dot{\Psi}(\beta_{\mathrm{T}}, \theta) = (1-\beta_{\mathrm{T}}^2 \sin^2\theta)^{p/2}[C \sin\{p(\omega-\pi)\} + D\cos\{p(\omega-\pi)\}] \tag{22}$$

and

$$\tan\varepsilon = (1-\beta_{\mathrm{L}}^2)^{1/2}\tan\theta \tag{23}$$

$$\tan\omega = (1-\beta_{\mathrm{T}}^2)^{1/2}\tan\theta \tag{24}$$

with $0 \leqslant (\omega, \varepsilon) \leqslant \pi$ if $0 \leqslant \theta \leqslant \pi$. Defining the displacement rate in the elastic unloading region as

$$\dot{u}_\gamma = Kv\dot{U}_\gamma^{\mathrm{el}}(\theta)r^{p-1} \tag{25}$$

where superscript el denotes the elastic solution, and comparing with eqn (5) an obvious condition is

$$s = p-1. \tag{26}$$

Using eqns (16), (6) and (7) one obtains

$$\dot{U}_1 = p\dot{\Phi}\cos\theta-(\dot{\Phi}')\sin\theta+p\dot{\Psi}\sin\theta+(\dot{\Psi}')\cos\theta \tag{27}$$

$$\dot{U}_2 = p\dot{\Phi}\sin\theta+(\dot{\Phi}')\cos\theta-p\dot{\Psi}\cos\theta+(\dot{\Psi}')\sin\theta. \tag{28}$$

Introduction of strain rates calculated from eqn (16) into the rate form of Hooke's law gives expressions for $\dot{\sigma}_{ij}$ as functions of the displacement rate potentials. From these equations the stresses follow as

$$\sigma_{11} = -\frac{\mu}{v}\left[\left(2+\beta_L^2\frac{\lambda}{\mu}\right)\frac{\partial\dot{\varphi}}{\partial x_1}+2\frac{\partial\dot{\psi}}{\partial x_2}\right]+f_1(x_2) \tag{29}$$

$$\sigma_{22} = -\frac{\mu}{v}\left[(\beta_T^2-2)\frac{\partial\dot{\varphi}}{\partial x_1}-2\frac{\partial\dot{\psi}}{\partial x_2}\right]+f_2(x_2) \tag{30}$$

$$\sigma_{12} = -\frac{\mu}{v}\left[2\frac{\partial\dot{\varphi}}{\partial x_2}+(\beta_T^2-2)\frac{\partial\dot{\psi}}{\partial x_1}\right]+f_3(x_2) \tag{31}$$

$$\sigma_{33} = \nu(\sigma_{11}+\sigma_{22})+f_4(x_2) \tag{32}$$

by using eqn (6) and an integration over x_1.

2.3. *Boundary and continuity conditions*

To complete the formulation of the problem, the governing equations in the plastic loading zone and the general form of the solution in the elastic unloading zone must be supplemented by boundary conditions at $\theta = 0$ and π, and continuity conditions at the boundaries between the different regions. Mode I symmetry ahead of the crack tip requires

$$\dot{U}_2(0) = \Sigma_{12}(0) = \dot{U}_1'(0) = \Sigma_{11}'(0) = \Sigma_{22}'(0) = \Sigma_{33}'(0) = 0. \tag{33}$$

On the crack surface σ_{22} and σ_{12} vanish, which means that

$$\Sigma_{22}(\pi) = \Sigma_{12}(\pi) = 0. \tag{34}$$

To determine the position of the boundary between the plastic loading region and the elastic unloading region an unloading condition is needed. At the unloading angle θ_1, $\dot{\sigma}_e = 0$. This gives by virtue of eqn (10)

$$-s\Sigma_e\cos\theta_1+\Sigma_e'\sin\theta_1 = 0. \tag{35}$$

When the angle θ_1 has been determined, four conditions at the boundary are needed to determine the four unknown constants A, B, C, D in the elastic solution. Because of residual plastic strains from the integration of eqn (13) the functions f_1, f_2, f_3, and f_4 in eqns (29)–(32) will in general be nonzero. However, it is possible to show, see Appendix A, that $f_2(x_2)$ and $f_3(x_2)$ vanish. This gives two conditions for the determination of A, B, C, D. The other

two conditions which are needed are continuity in displacement rates, as described in Appendix A.

When the constants in the elastic solutions have been determined it is possible to calculate values of Σ_{11} and Σ_{33} in the elastic unloading region from eqns (29) and (32). As mentioned above the values of the functions f_1 and f_4 will in general not vanish. The values of f_1 and f_4 at $\theta = \theta_1$ are denoted by $\Delta\sigma^r_{11}$ and $\Delta\sigma^r_{33}$, the first terms on the right-hand side of eqns (29) and (32) by σ^{el}_{11} and σ^{el}_{33} and the stresses by σ_{11} and σ_{33}. Observing that all stress fields are proportional to r^s and that f_1 and f_4 are functions of x_2 only, the actual values of σ_{11} and σ_{33} at $\theta \geqslant \theta_1$ in the elastic unloading region are

$$\sigma_{11} = \sigma^{el}_{11} + \Delta\sigma^r_{11}\left[\frac{\sin\theta}{\sin\theta_1}\right]^s \tag{36}$$

$$\sigma_{33} = \sigma^{el}_{33} + \Delta\sigma^r_{33}\left[\frac{\sin\theta}{\sin\theta_1}\right]^s. \tag{37}$$

Since this analysis includes the possibility of plastic reloading, it is necessary to have a condition for reloading. This condition also follows from the radial variation of the field variables and can be written as

$$\frac{\Sigma_e(\theta_1)}{(\sin\theta_1)^s} - \frac{\Sigma_e(\theta_2)}{(\sin\theta_2)^s} = 0 \tag{38}$$

where θ_2 is the angle at which plastic reloading occurs. The continuity condition at the plastic reloading boundary is that all elements in $\mathbf{y}$ are continuous. The derivatives $\mathbf{y}'(\theta_2)$ then follow immediately from eqn (13). Under some loading conditions there is a possibility for more than one unloading and/or one reloading. A second unloading angle will be denoted by θ_3 and a second reloading angle by θ_4. The conditions at these angles are of course the same as described above.

2.4. *Numerical integration*

In order to obtain solutions for the stress and velocity fields it is necessary to numerically integrate eqn (13). This is done by the same predictor–corrector algorithm as described by AKP. Since the matrix $\mathbf{D}$ in eqn (13) is singular at $\theta = 0$ the first step in the integration is done by a linear approximation of $\mathbf{y}(\theta)$

$$\mathbf{y}(\Delta\theta) \approx \mathbf{y}(0) + \mathbf{y}'(0)\Delta\theta \tag{39}$$

where $\Delta\theta$ is the step length of the increment in the θ-direction. The values of $\mathbf{y}$ and $\mathbf{y}'$ at $\theta = 0$ must then be known. These can be obtained by introducing Taylor expansions about $\theta = 0$ for $\mathbf{D}$, $\mathbf{R}$ and $\mathbf{y}$ in eqn (13), using eqn (33), and equating coefficients of θ^0 and θ^1 to zero. Before the start of the integration it is convenient to normalize the θ-variation by defining $\Sigma_e(0) = 1$ and to introduce

$$q = \Sigma_{11}(0)/\Sigma_{22}(0). \tag{40}$$

Expressions for $\mathbf{y}(0)$ and $\mathbf{y}'(0)$ are given in Appendix B. To determine the values of s and q it is necessary to iterate numerically. The procedure is started by guessing values of s and q. The solution $\mathbf{y}(\theta)$ is then obtained by integration of eqn (13) and also using the elastic solution for the unloading regions as described in the previous sections. At $\theta = \pi$ the values of Σ_{22} and Σ_{12} are checked to see whether they vanish. The iteration for s and q is performed by a modified Powell hybrid method, included in the subroutine C05NBF of the NAG subroutine library. Close to $\theta = \pi$ the values of $|\Sigma_{11}|$ and $|\Sigma_{33}|$ will tend to infinity. This is caused either by the fact that $\mathbf{D}$ in eqn (13) is singular at $\theta = \pi$, or by the singularity

Table 1. Plane strain (mode I) $\nu = 0.3$ (results from an analysis neglecting plastic reloading are given in parentheses)

α \ β	0.001	0.10	s 0.15	0.20	0.25
0.01	−0.080 (−0.090)				
0.02	−0.100 (−0.103)				
0.05	−0.144 (−0.141)	−0.106 (−0.104)			
0.10	−0.200 (−0.199)	−0.181 (−0.180)	−0.146 (−0.146)		
0.20	−0.303	−0.292	−0.276	−0.245	−0.161

α \ β	0.001	0.10	θ_1 0.15	0.20	0.25
0.01	135.37 (156.80)				
0.02	134.16 (149.25)				
0.05	131.10 (137.16)	121.69 (125.39)			
0.10	123.94 (125.10)	118.97 (119.84)	110.11 (110.43)		
0.20	114.21	112.71	110.77	107.78	103.45

α \ β	0.001	0.10	θ_2 0.15	0.20	0.25
0.01	145.61				
0.02	150.94				
0.05	161.16	167.81			
0.10	173.79	175.46	178.00		
0.20					

at $\theta = \pi$ of the second term on the right-hand side of eqns (36) and (37). However, Σ_{22} and Σ_{12} are well behaved near $\theta = \pi$ so the iteration for s and q described above meets no difficulties.

2.5. *Results*

The values of the singularity s, and of the respective unloading and reloading angles θ_1 and θ_2 are given, as functions of the hardening parameter α and the dimensionless crack tip velocity β, in Table 1. For comparison, the values calculated without plastic reloading on the crack flanks are given in parentheses. Observe that no plastic reloading occurs for values of the strain hardening parameter α, larger than α^*, where α^* is somewhere between 0.1 and 0.2. From an engineering point of view the most interesting results are those for small strain hardening. Most structural materials in which rapid crack propagation appears, do not exhibit large strain hardening. The results for higher values of α than 0.2 are not presented here but are in agreement with those reported by AKP.

A plot of the stress and velocity fields for $\alpha = 0.05$, $\beta = 0.1$, is shown in Fig. 3. The stresses and the velocities are normalized so that $\Sigma_e(\theta_1) = 1$.

3. PLANE STRAIN (MODE II)

3.1. *Formulation*

The formulation of the plane strain mode II problem is identical to the corresponding mode I problem except for the boundary conditions ahead of the crack tip. Mode II symmetry ahead of the crack tip requires

Table 2. Plane strain (mode II) $\nu = 0.3$

α \ β	0.001	0.10	s 0.15	0.20	0.25
0.01	−0.083	−0.079			
0.02	−0.114	−0.111	−0.108		
0.05	−0.172	−0.170	−0.168	−0.164	
0.10	−0.230	−0.229	−0.228	−0.226	−0.223
0.20	−0.303	−0.302	−0.302	−0.301	−0.298
α \ β	0.001	0.10	θ_1 0.15	0.20	0.25
0.01	26.07	26.53			
0.02	28.27	28.58	29.03		
0.05	31.61	31.85	32.17	32.66	
0.10	34.37	34.59	34.88	35.30	35.89
0.20	37.15	37.35	37.61	38.00	38.48
α \ β	0.001	0.10	θ_2, θ_3 0.15	0.20	0.25
0.01	179.97	179.97			
0.02	179.99	179.99	179.99		
0.05					
0.10					
0.20					127.44 133.59

$$\dot{U}_1(0) = \Sigma_{11}(0) = \Sigma_{22}(0) = \Sigma_{33}(0) = \Sigma'_{12}(0) = \dot{U}'_2(0) = 0. \tag{41}$$

Before integrating eqn (13) numerically, the θ-variation is normalized by $\Sigma_e(0) = 1$ and

$$q = \dot{U}_2(0)/\Sigma_{12}(0) \tag{42}$$

is introduced.

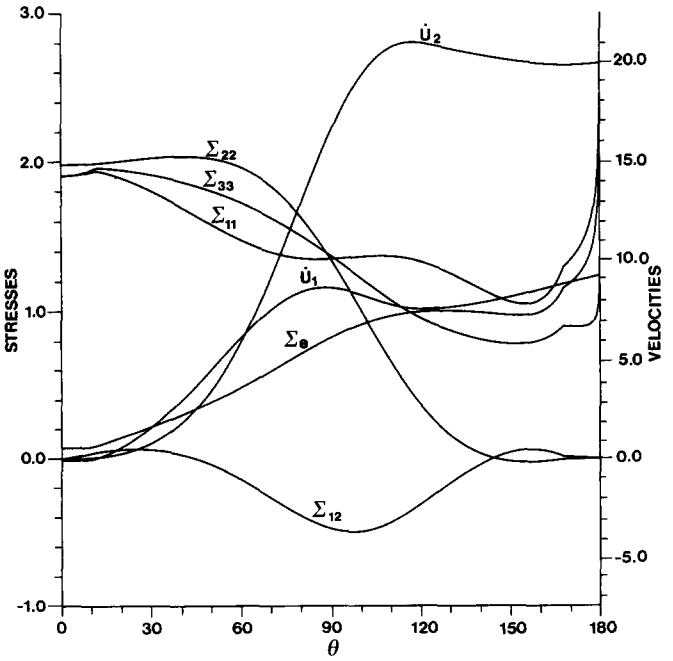

Fig. 3. Stress and velocity fields for plane strain (mode I), normalized such that $\Sigma_e(\theta_1) = 1$: $\alpha = 0.05$, $\beta = 0.1$.

Table 3. Plane stress (mode I) $\nu = 0.3$

α \ β	0.001	0.10	s 0.15	0.20	0.25
0.01	−0.086				
0.02	−0.119				
0.05	−0.178	−0.170	−0.157		
0.10	−0.237	−0.232	−0.225	−0.211	
0.20	−0.310	−0.306	−0.302	−0.292	−0.282
α \ β	0.001	0.10	θ_1 0.15	0.20	0.25
0.01	61.10				
0.02	64.45				
0.05	69.54	70.88	73.08		
0.10	73.65	74.75	76.25	78.74	
0.20	77.51	78.49	79.77	81.71	84.49

The values of $\mathbf{y}'(0)$ are obtained in the same way as for the mode I problem. The plane strain mode II boundary conditions are given in Appendix B. Given the values of $\mathbf{y}(0)$ and $\mathbf{y}'(0)$ the procedure described in Section 2.4 is used to iterate values of s and q.

3.2. *Results*

The results for the plane strain mode II formulation are given in Table 2. For this problem a second unloading appears for $\alpha = 0.2$, $\beta = 0.25$. The results of Ponte Castaneda (1987) show that for quasi-static conditions there will be a region of plastic reloading around $\theta = 130°$ for higher values of α. Evidently this region also appears for smaller α when the crack tip velocity increases.

Another interesting fact is that the values of the singularity parameter s and the unloading angle θ_1 are rather insensitive to the crack tip velocity given by β.

Stress and velocity fields for $\alpha = 0.05$, $\beta = 0.1$, are shown in Fig. 4. The results are normalized in the usual way by setting $\Sigma(\theta_1) = 1$.

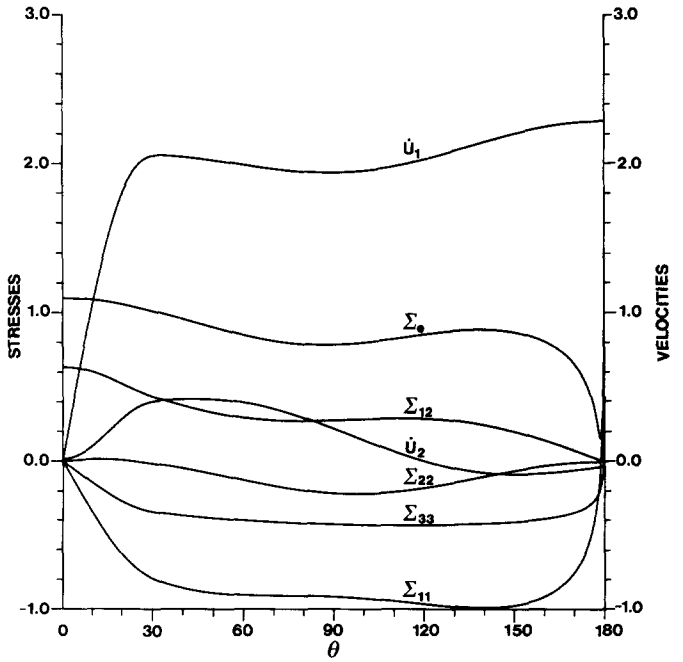

Fig. 4. Stress and velocity fields for plane strain (mode II), normalized such that $\Sigma_e(\theta_1) = 1$: $\alpha = 0.05$, $\beta = 0.1$.

Table 4. Plane stress (mode II) $\nu = 0.3$

α \ β	0.001	0.10	s 0.15	0.20	0.25
0.01	−0.080	−0.073			
0.02	−0.110	−0.106	−0.098		
0.05	−0.166	−0.163	−0.159	−0.151	
0.10	−0.219	−0.216	−0.212	−0.206	
0.20	−0.286	−0.283	−0.280	−0.275	−0.267

α \ β	0.001	0.10	θ_1, θ_2 0.15	0.20	0.25
0.01	31.92 179.91	32.92 179.91			
0.02	34.38 179.96	34.92 179.95	35.89 179.95		
0.05	38.01 114.87	38.28 113.03	38.62 111.95	39.10 112.04	
0.10	40.27 106.56	40.43 106.42	40.60 106.52	40.79 107.23	
0.20	42.44 102.63	42.58 102.63	42.73 102.74	42.94 103.13	43.19 104.04

α \ β	0.001	0.10	θ_3, θ_4 0.15	0.20	0.25
0.01					
0.02					
0.05	120.34 179.99	120.71 179.99	121.20 179.99	122.04 179.99	
0.10	123.50	123.79	124.19	124.90	
0.20	126.57	126.79	127.08	127.53	128.26

4. PLANE STRESS (MODE I)

4.1. *Formulation*

The plane stress mode I formulation is obtained by some slight changes of the formulation for the plane strain problem. The non-zero stresses are σ_{11}, σ_{22}, and σ_{12} $(= \sigma_{21})$. This means that in eqn (13) the last column in **D** and **R** and the last rows in **D**, **R**, **y** and **y**′ are deleted. The boundary conditions at $\theta = 0$ are also identical to the plane strain problem with the exception that $\Sigma_{33}(0) = \Sigma'_{33}(0) = 0$ and the consequences that follow from that.

The plane stress solution for the elastic unloading region can be obtained from the plane strain solution by replacing λ by $2\mu\nu/(1-\nu)$.

The iteration for values of s and q is equivalent to the procedure described in Section 2.4. When the solution is obtained it is renormalized in the usual ways such that $\Sigma_e(\theta_1) = 1$.

4.2. *Results*

The results for the plane stress mode I problem presented in Table 3 do not include any plastic reloading. For very small values of α Ponte Castaneda (1987) has obtained, in his quasi-static analysis, extremely small plastic reloading regions, but these have not been found in this work. This is probably an effect of using too large an increment $\Delta\theta$, in the integration of the governing equations. In Fig. 5, a plot of the stress and velocity fields for $\alpha = 0.05$, $\beta = 0.1$, is shown. The normalization of the stresses and the velocities is identical to that used in the previous sections.

5. PLANE STRESS (MODE II)

5.1. *Formulation*

The changes in the plane strain mode II formulation, to obtain the plane stress formulation, are identical to those changes described in the previous section for the mode I problem.

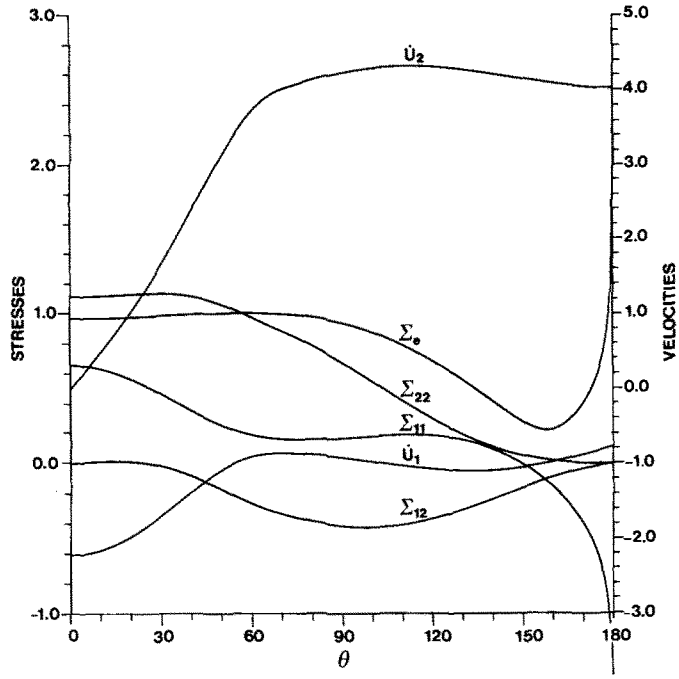

Fig. 5. Stress and velocity fields for plane stress (mode I), normalized such that $\Sigma_e(\theta_1) = 1$: $\alpha = 0.05$, $\beta = 0.1$.

5.2. *Results*

The plane stress mode II results presented in Table 4 include three different combinations of unloading and reloading angles. For low values of α an elastic unloading takes place at an angle just above $\theta = 30°$. Between this first unloading and a very narrow plastic reloading sector on the crack flank, the stress and velocity fields are governed by the elastic solution. For values of $\alpha > \alpha^*$, where α^* is between 0.05 and 0.10, no plastic reloading could be observed on the crack flank. Instead a sector of plastic reloading occurred just above $\theta = 100°$. In an intermediate zone around $\alpha \approx 0.05$, both the effects described above were observed. Stress and velocity fields for $\alpha = 0.05$, $\beta = 0.1$, are shown in Fig. 6. The normalization is identical to that described in previous paragraphs.

6. ANTIPLANE STRAIN (MODE III)

6.1. *Plastic loading region*

The mode III formulation for the plastic loading zone follows from AK. The stress and velocity fields are resolved into the same Cartesian coordinate system as was used in the previous sections (Fig. 1). The relevant displacement is $u_3(x_1, x_2, t)$ and the non-zero stresses are σ_{13} $(= \sigma_{31})$ and σ_{23} $(= \sigma_{32})$. For simplicity the following notation for the stresses and the strains is introduced:

$$\tau_\delta = \sigma_{\delta 3} \tag{43}$$

$$\gamma_\delta = 2\varepsilon_{\delta 3} = \partial u_3 / \partial x_\delta. \tag{44}$$

The governing system of differential equations is derived from the equation of motion

$$\tau_{\delta,\delta} = \rho \ddot{u}_3 \tag{45}$$

and the constitutive equations, which for plastic loading and J_2 flow theory are

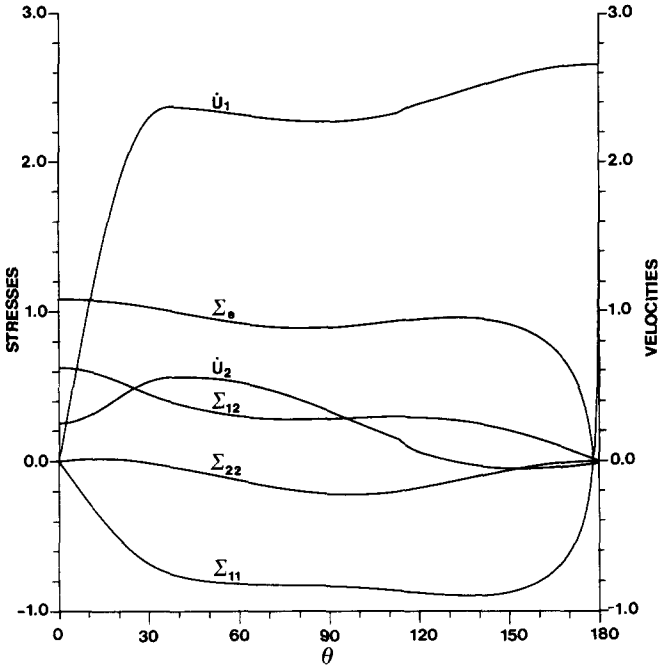

Fig. 6. Stress and velocity fields for plane stress (mode II), normalized such that $\Sigma_e(\theta_1) = 1$: $\alpha = 0.05$, $\beta = 0.1$.

$$\mu_t \dot{\gamma}_\delta = \alpha \dot{\tau}_\delta + (1-\alpha)\frac{\dot{\tau}_e}{\tau_e}\tau_\delta \tag{46}$$

where $\alpha = \mu_t/\mu$, μ is the shear modulus and μ_t the tangential stiffness of the bilinear stress–strain relation for stresses in excess of τ_0 (Fig. 2(b)). The effective stress τ_e is defined as

$$\tau_e = (\tau_1^2 + \tau_2^2)^{1/2}. \tag{47}$$

For the mode III problem a general solution of the form

$$\dot{u}_3 = Kv\dot{U}_3(\theta)r^s \tag{48}$$

is sought. The parameters K and v are defined in previous sections whereas $\dot{U}_3(\theta)$ and s are to be determined. Expressions for the stresses and stress rates are defined as

$$\{\tau_\delta, \tau_e\} = K\mu\{\Sigma_\delta(\theta), \Sigma_e(\theta)\}r^s \tag{49}$$

$$\{\dot{\tau}_\delta, \dot{\tau}_e\} = K\mu v\{\dot{\Sigma}_\delta(\theta), \dot{\Sigma}_e(\theta)\}r^{s-1}. \tag{50}$$

From eqns (6) and (7) it then follows that

$$\dot{\Sigma}_\delta = -s\Sigma_\delta \cos\theta + \Sigma'_\delta \sin\theta \tag{51}$$

and a similar expression results for $\dot{\Sigma}_e$. Equation (47) also gives

$$\Sigma_e = (\Sigma_1^2 + \Sigma_2^2)^{1/2}. \tag{52}$$

By using the same procedure as in Section 2.1, it is now possible to derive a system of non-linear differential equations from the equation of motion and the two constitutive relations

$$\mathbf{D}(\Sigma_\delta)\mathbf{y}' + \mathbf{R}\mathbf{y} = \mathbf{0} \tag{53}$$

where

$$\mathbf{y}^T = [\dot{U}_3, \Sigma_1, \Sigma_2]. \tag{54}$$

The elements of matrices **D** and **R** are given in Appendix B.

6.2. *Elastic unloading*

The mode III solution for the elastic unloading region follows from a slight generalization of Achenbach and Bazant (1975). It is possible to derive a solution of the form

$$u_3 = KU_3^{el}(\beta, \theta)r^p \tag{55}$$

where $\beta = v/C_T$, $C_T = (\mu/\rho)^{1/2}$ and $U_3^{el}(\beta, \theta)$ may be written as

$$U_3^{el}(\beta, \theta) = (1-\beta^2 \sin^2 \theta)^{p/2}[A \sin \{p(\omega-\pi)\} + B \cos \{p(\omega-\pi)\}]. \tag{56}$$

In eqn (55), A and B are two constants which are determined by continuity conditions at the boundary between plastic loading and elastic unloading. The angle ω is related to θ through

$$\tan \omega = (1-\beta^2)^{1/2} \tan \theta \tag{57}$$

with $0 \leqslant \omega \leqslant \pi$ if $0 \leqslant \theta \leqslant \pi$.

If the displacement rate in the elastic region is defined as

$$\dot{u}_3^{el} = Kv\dot{U}_3^{el}(\theta)r^{p-1} \tag{58}$$

then $\dot{U}_3^{el}(\theta)$ follows from eqns (55), (56), (6) and (7) as

$$\dot{U}_3^{el}(\theta) = -[p \cos \theta U_3^{el} - \sin \theta (U_3^{el})']. \tag{59}$$

An obvious condition is obtained if eqn (48) is compared with eqn (58)

$$s = p-1. \tag{60}$$

The elastic shear stresses τ_δ can be calculated as

$$\tau_\delta = \mu \frac{\partial u_3^{el}}{\partial x_\delta}. \tag{61}$$

Inserting eqn (55) into eqn (61) and comparing with eqn (49) gives the following expressions for Σ_1^{el} and Σ_2^{el}:

$$\Sigma_1^{el} = [p \cos \theta U_3^{el} - \sin \theta (U_3^{el})'] \tag{62}$$

$$\Sigma_2^{el} = [p \sin \theta U_3^{el} + \cos \theta (U_3^{el})']. \tag{63}$$

6.3. *Boundary and continuity conditions*

Mode III symmetry ahead of the crack tip requires that

$$\dot{U}_3(0) = \Sigma_1(0) = \Sigma_2'(0) = 0. \tag{64}$$

Since $\sigma_{23} = 0$ on the crack surface, it follows that

Table 5. Antiplane strain (mode III) (results from an analysis neglecting plastic reloading are given in parentheses)

α \ β	0.001	0.10	s 0.15	0.20	0.25
0.01	−0.073 (−0.074)	−0.067 (−0.067)			
0.02	−0.101 (−0.101)	−0.097 (−0.097)	−0.091 (−0.091)		
0.05	−0.153	−0.151	−0.147	−0.141	
0.10	−0.207	−0.205	−0.203	−0.199	−0.194
0.20	−0.277	−0.276	−0.274	−0.272	−0.268
α \ β	0.001	0.10	θ_1 0.15	0.20	0.25
0.01	52.88 (52.88)	54.16 (54.16)			
0.02	57.21 (57.21)	57.87 (57.87)	58.97 (58.97)		
0.05	63.98	64.41	64.96	65.79	
0.10	69.82	70.18	70.64	71.28	72.11
0.20	76.08	76.41	76.82	77.39	78.11
α \ β	0.001	0.10	θ_2 0.15	0.20	0.25
0.01	179.95	179.95			
0.02	179.98	179.98	179.98		
0.05					
0.10					
0.20					

$$\Sigma_2(\pi) = 0. \tag{65}$$

To determine the position where elastic unloading occurs, eqn (35) is applicable. To specify the elastic solution, two continuity conditions for the determination of A and B are needed. By a procedure similar to the one described in Appendix A, it is possible to show that these two conditions are continuity in displacement rate and that Σ_2 obtained from the numerical integration of eqn (53) and from the elastic solution (63) are identical. The values of the remaining stress Σ_1 calculated from the numerical integration and from eqn (62) respectively, will in general, not be the same. In order to obtain the actual stress Σ_1 in the unloading region, including the residual stress, the same procedure as in eqns (36) and (37) has to be applied.

The condition for plastic reloading and the continuity conditions at the boundary where reloading takes place are identical with those described at the end of Section 2.3.

6.4. *Numerical integration*

To numerically integrate eqn (53) the same algorithm as was described in Section 2.4 is used. The singularity of matrix $\mathbf{D}$ at $\theta = 0$ requires both $\mathbf{y}(0)$ and $\mathbf{y}'(0)$. They are obtained by a Taylor expansion of eqn (53) around $\theta = 0$. The result is presented in Appendix B. A simplifying fact for the mode III problem is that there is only one undetermined parameter, s, which is determined by numerical iteration. Although the value of Σ_1 is singular at $\theta = \pi$, the iteration meets no difficulties since Σ_2 is well behaved near $\theta = \pi$.

6.5. *Results*

The results for the antiplane strain mode III problem presented in Table 5 are rather insensitive to plastic reloading. For values of $\alpha < \alpha^*$, where α^* is between 0.02 and 0.05, narrow sectors of plastic reloading were observed on the crack flank. However, the size of the sector was in no case larger than 0.1° for the results presented in this paper. These small zones did not affect the singularity nor the stress and velocity fields to any large extent. An

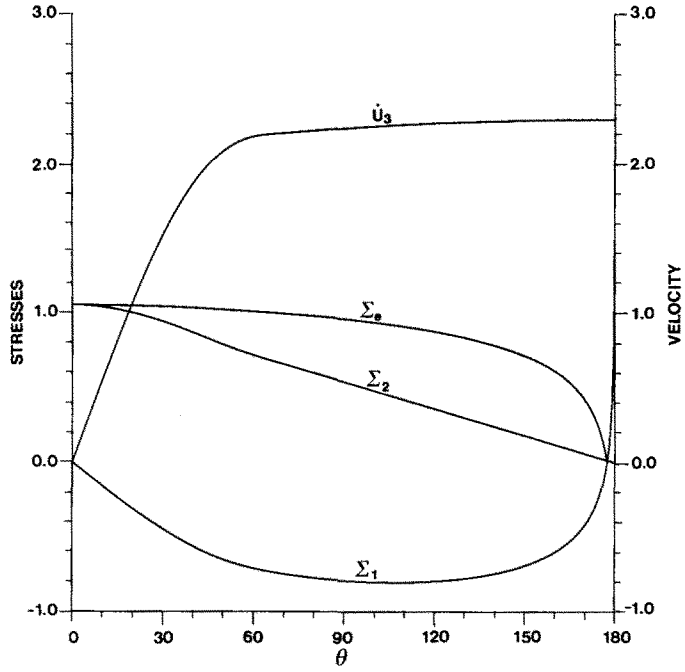

Fig. 7. Stress and velocity fields for antiplane strain (mode III), normalized such that $\Sigma_e(\theta_1) = 1$: $\alpha = 0.05$, $\beta = 0.1$.

example of the stress and velocity fields for $\alpha = 0.05$, $\beta = 0.1$, is presented in Fig. 7. The fields are normalized in the usual way.

7. DISCUSSION

All of the results presented in this paper were calculated for $\nu = 0.3$. This enables comparisons to be made between the different loading conditions. A first observation is that the value of the singularity s is more sensitive to α than to the type of loading. The singularity is also rather independent of β for modes II and III. For mode I, on the other hand, the strength of the singularity decreases with increasing crack tip velocity. This effect is more pronounced close to the limit speed, especially for the plane strain formulation. Although the singularity is rather insensitive to β for mode II, the other unknown parameter, q, shows a larger variation when β is changed.

Another observation is that the values of α and β, for which calculations can be performed with the present formulation, are almost identical for modes II and III, but mode I has a lower limit speed for a given value of α. This indicates that the limit speed for mode II, as is for mode III is ruled by the quasi-shear wave speed, in which E is replaced by E_t, but not the quasi-Rayleigh wave speed as in the mode I formulation.

A conclusion which can be drawn from this work is that plastic reloading does not play an important role concerning the asymptotic crack tip fields for linear strain hardening materials with large hardening. An exception is the mode II formulation where plastic reloading must be included in order to obtain accurate results. For low values of the hardening parameter α, plastic reloading on the crack flank must be taken into account, especially for the mode I plane strain formulation.

Further research in this area should include investigations of crack tip speeds above the limit speed. So far only results obtained by the finite element method are available.

REFERENCES

Achenbach, J. D. and Bazant, Z. P. (1975). Elastodynamic near tip stress and displacement fields for rapidly propagating cracks in orthotropic materials. *J. Appl. Mech.* **42**, 183–189.

Achenbach, J. D. and Dunayevsky, V. (1981). Fields near a rapidly propagating crack tip in an elastic–perfectly plastic material. *J. Mech. Phys. Solids* **29,** 283–303.
Achenbach, J. D. and Kanninen, M. F. (1978). Crack-tip plasticity in dynamic fracture mechanics. In *Fracture mechanics* (Edited by N. Perrone, H. Liebowitz, D. Mulville and W. Pilkey), pp. 649–670. University of Virginia Press, Charlottesville, Virginia.
Achenbach, J. D., Burgers, P. and Dunayevsky, V. (1979). Near-tip plastic deformations in dynamic fracture problems. In *Nonlinear and Dynamic Fracture* (Edited by N. Perrone and S. Atluri), AMD-Vol. 35, pp. 105–124. American Society of Mechanical Engineers, New York.
Achenbach, J. D., Kanninen, M. F. and Popelar, C. H. (1981). Crack tip fields for fast fracture of an elastic–plastic material. *J. Mech. Phys. Solids* **29,** 211–225.
Lo, K. K. (1982). Elastic–plastic field at the tip of a propagating shear crack. *Q. Appl. Math.* **40,** 27–36.
Lam, P. S. and Freund, L. B. (1985). Analysis of dynamic growth of a tensile crack in an elastic–plastic material. *J. Mech. Phys. Solids* **33,** 153–167.
Leighton, J. T., Champion, C. R. and Freund, L. B. (1987). Asymptotic analysis of steady dynamic crack growth in an elastic–plastic material. *J. Mech. Phys. Solids* **35,** 541–563.
Ponte Castaneda, P. (1987). Asymptotic field in steady crack growth with linear strain-hardening. *J. Mech. Phys. Solids* **35,** 227–268.
Slepyan, L. I. (1976). Crack dynamics in an elastic–plastic body. *Izv. Akad. SSSR, Mekh. Tverdogo Tela* **11,** 144–153.

APPENDIX A

Stresses in the elastic unloading region

The stresses which follow from the formulation in the elastic unloading region are given in eqns (29)–(32). In a simplified notation they can be written as

$$\sigma_{ij} = g_{ij}(A, B, C, D) + h_{ij}(x_2) \tag{A1}$$

where A, B, C, D are the constants in eqns (21) and (22) and h_{ij} are the functions f_1, f_2, f_3 and f_4. The acceleration $\ddot{u}_i$ can be expressed in the constants A, B, C, D by using eqn (16)

$$\ddot{u}_i = v^2 \frac{\partial^2 u_i}{\partial x_1^2} = k_i(A, B, C, D). \tag{A2}$$

By introducing eqns (A1) and (A2) into the equations of motion

$$\sigma_{ij,j} = \rho v^2 \frac{\partial^2 u_i}{\partial x_1^2} \tag{A3}$$

one obtains

$$g_{ij,j} + h_{ix_2,x_2} = \rho k_i. \tag{A4}$$

From the general solution it is known that the terms $g_{ij,j}$ exactly balance ρk_i, thus

$$h_{ix_2,x_2} = 0 \tag{A5}$$

and

$$h_{ix_2} = 0. \tag{A6}$$

A comparison of eqns (A1), (A6) and (29)–(32) then gives that the functions f_2 and f_3 in eqns (30) and (31) vanish.

Continuity in displacement rate at unloading

If discontinuities in the stresses and the displacement rates exist across the boundary $\theta = \theta_1$, then they must satisfy the following equation:

$$[\sigma_{ij} n_j] = -\rho v \sin \theta_1 [\dot{u}_i]. \tag{A7}$$

The displacements will always be continuous. Through the steady state assumption, the displacement rates can be expressed by spatial derivatives of the displacements. The only possibilities for discontinuities in displacement derivatives are $[\partial v_r/\partial\theta]$ and $[\partial v_\theta/\partial\theta]$. Thus

$$[\dot{u}_i] = f_i\left(\left[\frac{\partial v_r}{\partial\theta}\right], \left[\frac{\partial v_\theta}{\partial\theta}\right]\right) \tag{A8}$$

where f_i is a linear function of its arguments.

Continuity in plastic strains across $\theta = \theta_p$ implies that

$$[\sigma_{ij}] = C_{ijkl}[\varepsilon_{kl}] \tag{A9}$$

where Hooke's law has been summarized in the constants C_{ijkl}.

The discontinuities in strains can be expressed as linear functions of $[\partial v_r/\partial\theta]$ and $[\partial v_\theta/\partial\theta]$. The two equations (A7) and the four non-trivial equations (A9) will then constitute a homogeneous linear equation system for the six unknowns: $[\sigma_{rr}]$, $[\sigma_{\theta\theta}]$, $[\sigma_{r\theta}]$, $[\sigma_{zz}]$, $[\partial v_r/\partial\theta]$, $[\partial v_\theta/\partial\theta]$. For the crack tip velocities considered in this report, the only possible solution is that all unknowns are equal to zero. Thus, the displacement rates and the stresses are continuous across $\theta = \theta_1$.

APPENDIX B

The boundary conditions at $\theta = 0$ for the plane strain (mode I) problem are

$$\mathbf{y}^{\mathrm{T}}(0) = \Sigma^{-1}[a, 0, q, 1, 0, g] \tag{B1}$$

$$\mathbf{y}'^{\mathrm{T}}(0) = \Sigma^{-1}[0, b, 0, 0, c, 0] \tag{B2}$$

where

$$a = (g+1)\left[\frac{1-\alpha}{2\alpha}+\nu\right]-\frac{q}{\alpha} \tag{B3}$$

$$b = s(g+q)\left[\frac{1-\alpha}{2\alpha}+\nu\right]-\frac{s}{\alpha} \tag{B4}$$

$$c = -s(\beta^2 a+q) \tag{B5}$$

$$g = \alpha(q+1)\left[\frac{1-\alpha}{2\alpha}+\nu\right] \tag{B6}$$

$$\Sigma = (1+q^2+g^2-q-qg-g^2). \tag{B7}$$

The plane stress (mode I) boundary conditions are obtained from eqns (B1)–(B7) by setting $g = 0$ and deleting the last row of $\mathbf{y}(0)$ and $\mathbf{y}'(0)$.

The plane strain (mode II) boundary conditions at $\theta = 0$ are

$$\mathbf{y}^{\mathrm{T}}(0) = \Sigma^{-1}[0, q, 0, 0, 1, 0] \tag{B8}$$

$$\mathbf{y}'^{\mathrm{T}}(0) = \Sigma^{-1}[b, 0, d, a, 0, c] \tag{B9}$$

where

$$a = -s(1+q\beta^2) \tag{B10}$$

$$b = -s\left[q+2(1+\nu)+\frac{3(1-\alpha)}{\alpha}\right] \tag{B11}$$

$$c = \frac{m}{(1-s/\alpha)^2-m^2}[b(1-s)+a(m-(1-s/\alpha))] \tag{B12}$$

$$d = -a-c\frac{\alpha-s}{\alpha m} \tag{B13}$$

$$m = -\nu+s\left(\frac{1-\alpha}{2\alpha}+\nu\right) \tag{B14}$$

$$\Sigma = \sqrt{3}. \tag{B15}$$

The elements of matrices $\mathbf{D}$ and $\mathbf{R}$ for the antiplane strain (mode III) problem are

$$\left.\begin{aligned}
D_{11} &= \beta^2 \sin\theta \\
D_{12} &= D_{21} = \sin\theta \\
D_{13} &= D_{31} = -\cos\theta \\
D_{22} &= \sin\theta\left[1+\frac{1-\alpha}{\alpha}\frac{\Sigma_1^2}{\Sigma_e^2}\right] \\
D_{23} &= D_{32} = \frac{1-\alpha}{\alpha}\frac{\Sigma_1\Sigma_2}{\Sigma_e^2}\sin\theta \\
D_{33} &= \sin\theta\left[1+\frac{1-\alpha}{\alpha}\frac{\Sigma_2^2}{\Sigma_e^2}\right]
\end{aligned}\right\} \tag{B16}$$

$$\left.\begin{aligned} R_{11} &= -s\beta^2 \cos\theta \\ R_{12} &= R_{21} = -s\cos\theta \\ R_{13} &= R_{31} = -s\sin\theta \\ R_{22} &= R_{33} = -\frac{s\cos\theta}{\alpha} \\ R_{23} &= R_{32} = 0. \end{aligned}\right\} \tag{B17}$$

The boundary conditions at $\theta = 0$ for the mode III problem are

$$\mathbf{y}^{\mathrm{T}}(0) = [0, 0, 1] \tag{B18}$$

$$\mathbf{y}'^{\mathrm{T}}(0) = \left[-\frac{s}{\alpha}, \frac{s(s-1)}{\alpha - s}, 0\right]. \tag{B19}$$